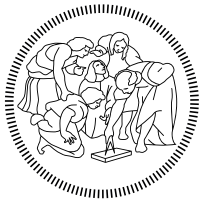

POLITECNICO
MILANO 1863

Effect of Area C Introduction: Expansion on PM10 and PM2.5 concentrations

Bayesian Statistics Project

Gutierrez Miguel
Luca Alessandra
Maiocchi Ester
Mazza Marianna
Sottanella Amedeo
Travaglini Federico

Tutor: Colombara Simone and Beltramin Giulio
Professor: Guglielmi Alessandra

February 19, 2026

Contents

1 Introduction

Air pollution represents a major environmental and public health concern for large metropolitan areas, Milan is no exception. As one of the most densely populated and industrialized cities in Italy, Milan frequently experiences elevated levels of atmospheric pollutants, such as particulate matter. Here, we investigated whether the introduction of Area C, a central restricted traffic zone implemented in January 2012, led to a measurable reduction in air pollution levels within the city. Then, we analyzed pollution concentrations across the whole Lombardy region.

Our analysis focused on particulate matter concentrations, specifically PM10 and PM2.5, which are among the most harmful pollutants due to their well-known adverse health effects. In addition to examining pollutant levels directly, we accounted for their relationship with weather conditions.

2 Preliminary Data Analysis

2.1 Data Preprocessing

Our dataset is obtained by merging two sources:

- Daily measurements of PM10 and PM2.5 collected from 2010 to 2017 by ARPA Milan air-quality monitoring stations (inside and outside Area C). [4, 5]
- Daily recordings of weather conditions from the website Open-Meteo (wind speed, temperatures and rain). [3]

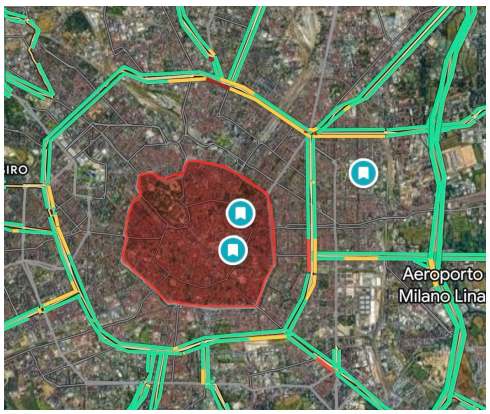

Figure 1: Area C corresponds to the central area of Milan, denoted by the red region while the blue and white circles indicate the ARPA stations.

To better manage the amount of data, we aggregated the daily recordings in weekly ones, using different approaches for each variable:

- **Pollutants:** weekly mean when we had at least 30% of valid daily measurements and NA otherwise, we then interpolated the data to fill the missing values;

- **Temperature:** weekly maximum of $T_{\max}$ and weekly minimum of $T_{\min}$ to represent the weekly range;
- **Rain:** sum of daily precipitations;
- **Wind:** weekly maximum wind speed.

After checking data availability, we restricted our attention to a small set of sensors that are informative for Area C and have adequate coverage throughout the whole time range: sensors `6956`, `10273`, and `10283`. We also introduced an 'inside Area C' indicator to denote whether a sensor is inside Area C.

PM2.5 measurements are only available for one sensor (10283), thus spatial inference on PM2.5 would not guarantee a reliable control structure. For this reason, we only focused on PM10 and built the modeling dataset using:

- **Inside Area C (target):** PM10 from sensor 6956;
- **Outside Area C (control):** PM10 from sensor 10273;
- **Weather covariates:** $T_{\max}$, $T_{\min}$, rain, wind.

2.2 Exploratory data analysis

We then plot the main covariates (temperatures, rain and wind) and the pollutant time series for the sensor inside Area C to determine their behaviour and correlation.

Temperature. Figure 2 shows weekly maximum (red) and minimum (blue) temperatures. The seasonal pattern is very strong and regular across years, which suggests that any pollution model should explicitly account for seasonality, either through a seasonal component or through temperature covariates.

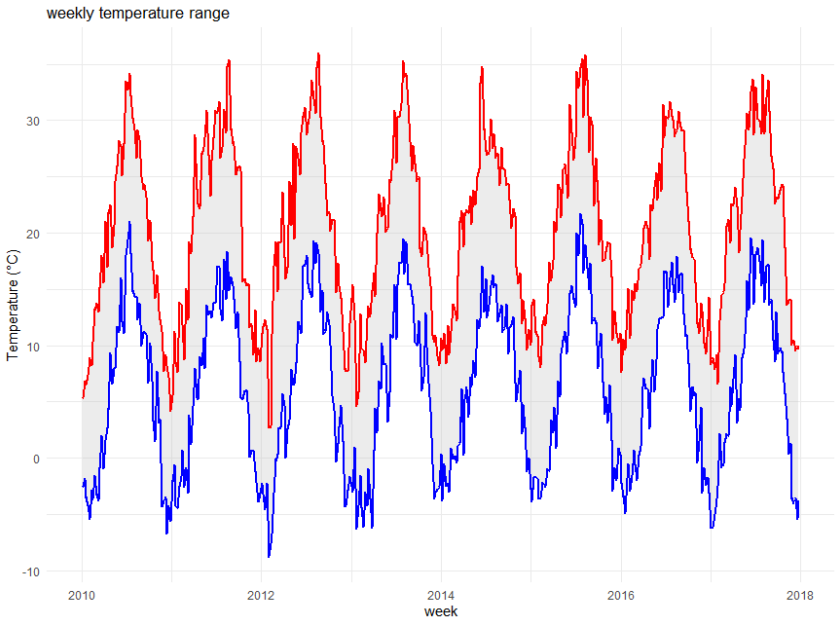

Figure 2: Weekly temperature range: $T_{\max}$ (red) and $T_{\min}$ (blue).

Rain. Figure 3 shows weekly total rainfall. Rain is intermittent: many weeks have small values and a few weeks have very large spikes. Milan's irregular rain behaviour suggests it might have a non-smooth influence on air pollution.

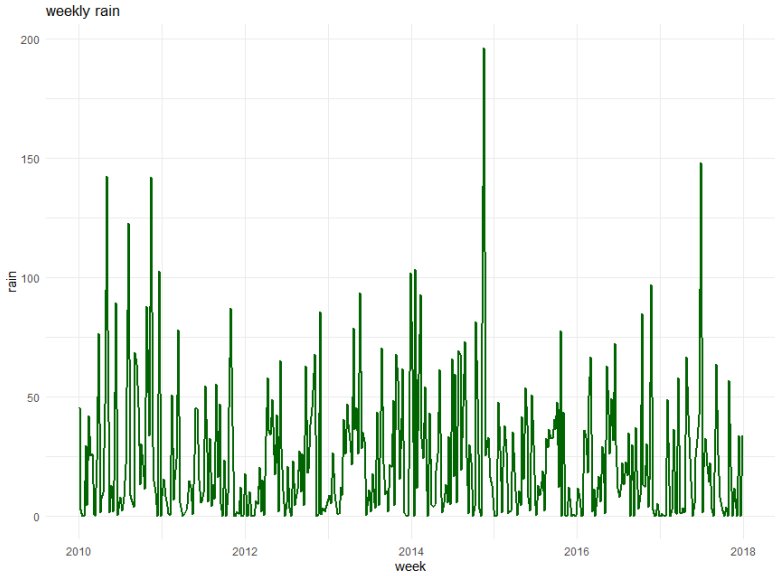

Figure 3: Weekly rain.

PM10. Figure 4 shows the plot of the weekly PM10 levels for the sensor inside Area C. At first sight, it appears that the intervetion in 2012 decreased the levels of pollution. Moreover, the PM10 time series shows a recurring pattern, with apparent winter peaks and summer lows, and occasional sharp peaks.

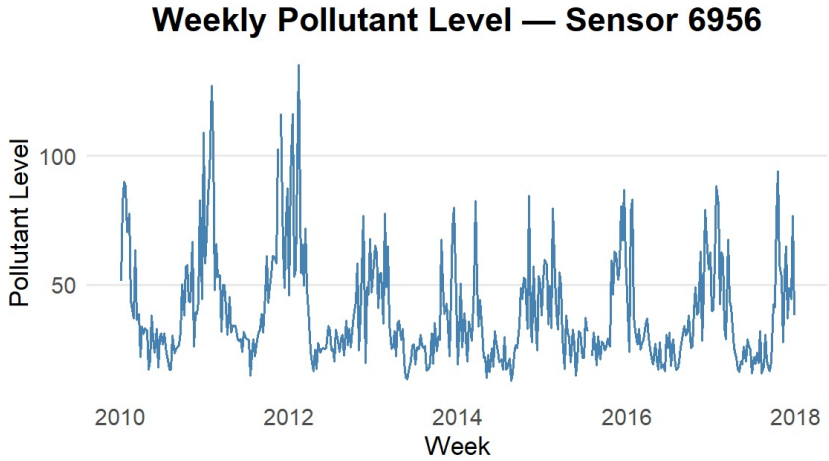

Figure 4: Weekly pollutant level for sensor 6956 (inside Area C).

As a final exploratory step, we computed the correlation matrix among the target time series and covariates (Figure 5). Two results were especially relevant:

- The inside and outside PM10 series are **strongly correlated** ($\rho \approx 0.95$);

- PM10 inside Area C has **negative correlations** with temperature and also very weak negative correlation with rain and wind. This is coherent with the intuition that colder weeks should have higher PM10, while precipitation and ventilation reduce pollution.

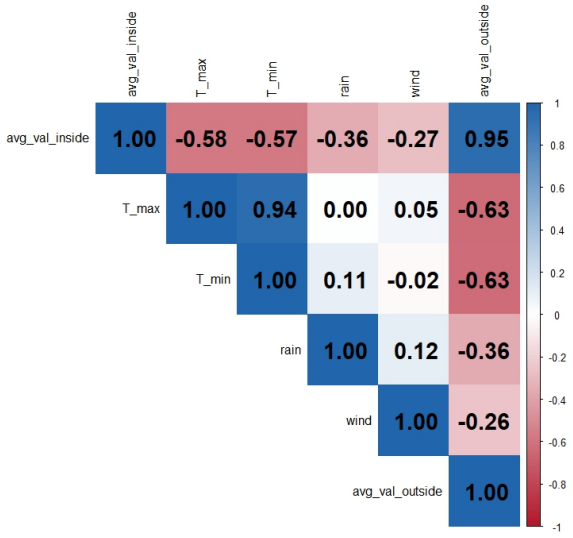

Figure 5: Correlation heatmap between PM10 inside/outside and weather covariates.

3 Causal Impact Model for Milan

In order to investigate the effect of the introduction of Area C, we used the Causal Impact package [2], which is based on a Bayesian Structural Time Series (BSTS) model. The main idea is to fit a time-series model on the *pre-intervention* period and then use it to predict the *counterfactual* trajectory in the *post-intervention* period (i.e., what would have happened without the introduction of the policy). The causal effect is obtained by comparing the observed series with this counterfactual prediction.

3.1 Observed series and intervention setup

Let $t = 1, \dots, m$ index the full time period and let $n < m$ be the time index of the intervention. We split the data into:

- **Training (pre-intervention) period** $t = 1, \dots, n$;
- **Post-intervention period** $t = n + 1, \dots, m$.

The model is fitted using $y_{1:n}$ (together with covariates $x_{1:n}$). Then, using the fitted model and the covariates $x_{n+1:m}$, we generated the counterfactual predictions $\tilde{y}_{n+1:m}$ for the post period.

3.2 Our model

Observation model. We used an additive model with three parts: baseline level (trend), seasonality, and regression on covariates.

$$y_t \mid \mu_t, \gamma_t, \boldsymbol{\beta}, \sigma_\varepsilon^2 \overset{\text{ind}}{\sim} \mathcal{N}\big(\mu_t + \gamma_t + \mathbf{x}_t^\top \boldsymbol{\beta},\ \sigma_\varepsilon^2\big)\,, \tag{1}$$

where:

- $t = 1, \ldots, n$ is the week index;
- μ_t is the local linear level (baseline trend);
- γ_t is the seasonal component;
- $\mathbf{x}_t$ contains the covariates values (weather and control sensor);
- $\boldsymbol{\beta}$ contains the regression coefficients;
- σ_ε^2 is the observation noise variance.

Trend component. We modeled the baseline trend as a random walk:

$$\mu_{t+1} = \mu_t + \eta_{\mu,t}, \qquad \eta_{\mu,t} \sim \mathcal{N}(0, \sigma_\mu^2). \qquad t = 1, ..., n \tag{2}$$

Intuitively, this allows the series to slowly drift over time (for example due to long-term changes in emissions or measurement conditions), instead of forcing a fixed global trend.

Seasonal component. Since we worked with weekly data, we included an annual seasonal pattern with period $S = 52$ weeks. Using the standard structural seasonality formulation:

$$\gamma_{t+1} = -\sum_{s=0}^{S-2} \gamma_{t-s} + \eta_{\gamma,t}, \qquad \eta_{\gamma,t} \sim \mathcal{N}(0, \sigma_\gamma^2). \qquad t = 1, ..., n \tag{3}$$

The negative sum constraint ensures that seasonal effects over one full cycle sum to zero, avoiding identifiability issues.

Regression component. A crucial part of Causal Impact is the regression on *contemporaneous* control series and covariates. The main assumption is that these controls are not affected by the intervention itself (no spillover), and that the relationship observed between treated and control series in the pre-period remains approximately valid in the post-period.

In our case we used a static regression:

$$\mathbf{x}_t^\top \boldsymbol{\beta} = \beta_1 T_{\max,t} + \beta_2 T_{\min,t} + \beta_3 \text{rain}_t + \beta_4 \text{wind}_t + \beta_5\, y_t^{\text{outside}}, \qquad t = 1, ..., n \tag{4}$$

where y_t^{outside} represents the PM10 series from a sensor outside Area C. The choice to include y_t^{outside} was motivated by the strong correlation between inside and outside PM10 observed in the exploratory analysis.

Prior. The dynamics of most state components depend on their diffusion variances, which control the rate at which these components change over time. Following the standard approach, we placed Gamma priors on inverse variances:

$$\frac{1}{\sigma_\mu^2},\ \frac{1}{\sigma_\gamma^2},\ \frac{1}{\sigma_\varepsilon^2} \overset{\text{ind}}{\sim} \text{Gamma}\left(\frac{\nu_i}{2}, \frac{s_i^2}{2}\right), \qquad i \in \{\mu, \gamma, \varepsilon\}. \tag{5}$$

Since we have multiple covariates, we can use a spike-and-slab prior to encourage sparsity and avoid overfitting. $(j = 1, \ldots, 5)$

$$\beta_j \mid \gamma_j \overset{\text{ind}}{\sim} (1 - \gamma_j)\, \delta_0 + \gamma_j\, \mathcal{N}\left(0, \sigma_{\beta_j}^2\right) \tag{6}$$

$$\gamma_j \mid \theta_j \overset{\text{ind}}{\sim} \text{Be}(\theta_j) \tag{7}$$

$$\theta_j \overset{\text{ind}}{\sim} \pi(\theta_j) \tag{8}$$

Intuitively: some coefficients are allowed to be exactly zero (the "spike"), while the non-zero ones follow a weak Gaussian prior (the "slab"). This lets the model average over different sets of covariates instead of us manually choosing them.

Causal effect and summary measures. Given posterior predictive samples $\tilde{y}_t^{(\tau)}$ for $t > n = 106$, we defined the pointwise impact (for each posterior draw τ) as:

$$\phi_t^{(\tau)} = y_t - \tilde{y}_t^{(\tau)}, \qquad t = n + 1, \ldots, 416. \tag{9}$$

From these samples we obtained posterior summaries such as the posterior mean impact and credible intervals. To understand the overall total effect over the post-intervention period, we considered the cumulative impact over the pollutant:

$$\Phi_t^{(\tau)} = \sum_{t'=n+1}^{t} \phi_{t'}^{(\tau)}, \qquad t = n + 1, \ldots, 416. \tag{10}$$

We created a visual representation of this in the cumulative plot in Figure 6.

3.3 Implementation

Area C was officially introduced on January 16, 2012. Therefore, we split the time range into:

- **Pre-intervention period:** from 2010-01-01 to 2012-01-15;
- **Post-intervention period:** from 2012-01-16 to 2017-12-31.

The model is trained only on the pre-intervention segment. Then, keeping the covariates observed in the post-period, the model generates a posterior predictive distribution for the counterfactual $\tilde{y}_t$ (what PM10 inside Area C would have looked like without the intervention).

3.3.1 Model configuration

We implemented two model configurations:

- **Baseline model:** the standard CausalImpact specification using the covariates provided in the input table without the trend and seasonality components;
- **Advanced model (final choice):** a model that explicitly includes weekly seasonality with annual period. We also increased the number of MCMC iterations to 5000 and used a small prior scale for the local level component to regularize the baseline level and avoid overly volatile trends.

The seasonal configuration is motivated by the clear yearly pattern observed in PM10 and temperatures in the exploratory analysis.

3.4 Results

Figure 6 shows the results obtained with CausalImpact package, the plot consists of three panels:

- **Observed Data and Counterfactual (Top plot):** this plot illustrates the observed y_t (black line) and the model prediction within the 95% confidence intervals (blue band). The vertical dashed line indicates the start of the post-intervention period. A good sign is that the model tracks the observed series reasonably well in the pre-period;
- **Pointwise Impact (Middle plot):** the estimated effect $\phi_t = y_t - \tilde{y}_t$ for each week, together with its 95% credible interval. Values below zero indicate that observed PM10 is lower than the counterfactual prediction (a reduction);
- **Cumulative Impact (Bottom plot):** the cumulative sum of pointwise effects over time. A decreasing curve suggests an overall negative cumulative effect, meaning a reduction in pollution relative to the counterfactual.

Figure 6: CausalImpact results.

To better understand the results we focused on the cumulative plot: it appears that the introduction of Area C had an impact on pollution levels since the curve is decreasing and the credible interval does not include zero.

3.5 Stan Model for Causal Impact

We wanted to closely replicate the structure of the BSTS model used by the CausalImpact function. The model is built on the pre-intervention data, capturing the temporal evolution of the series via a local level following a random walk and a weekly seasonal component. Regressions on external covariates (weather and PM10 levels) are included in a static way, and all noise scales and regression coefficients are assigned weakly informative priors to ensure numerical stability and identifiability.

After fitting the model to the pre-intervention period, we simulated forward the series for the post-intervention period using the same state evolution equations and the observed post-period covariates. These simulations generated the counterfactuals and allowed us to compute both pointwise and cumulative impacts of the intervention, analogous to the original CausalImpact function.

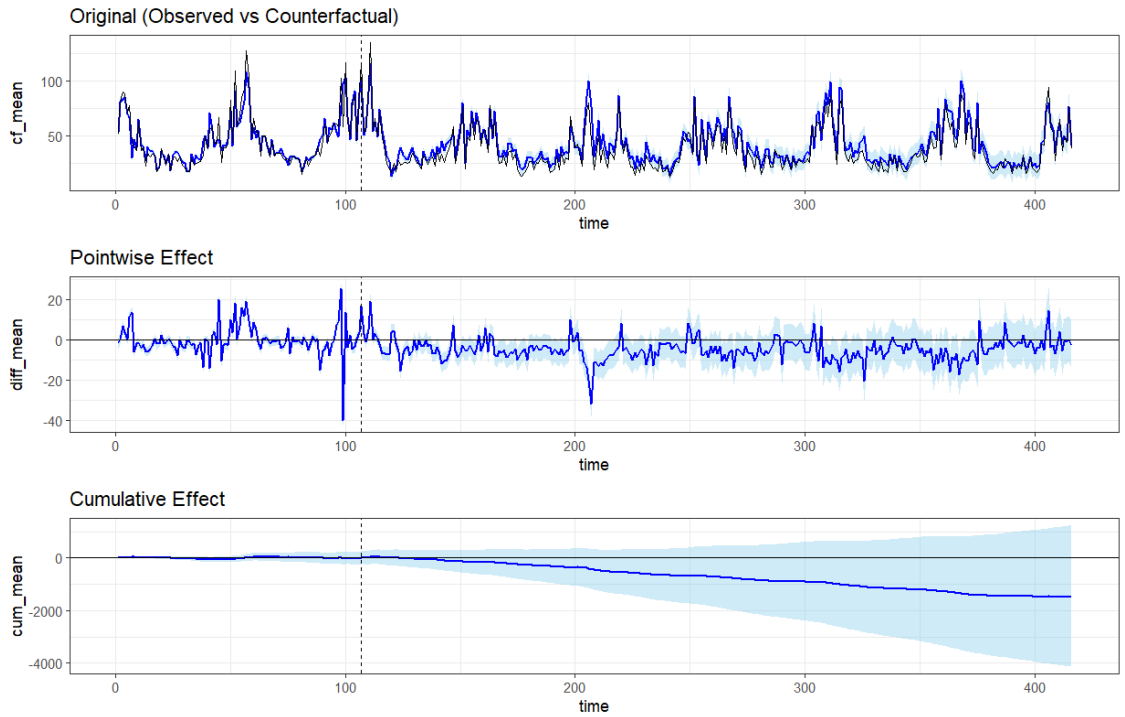

Figure 7: CausalImpact with Stan results. Top: observed series and counterfactual prediction. Middle: pointwise impact. Bottom: cumulative impact. The dashed vertical line marks the start of the post-intervention period (2012-01-16).

To evaluate the consistency of the estimated intervention effect, we compared the results obtained using the CausalImpact framework with those produced by the Stan model. While the point estimates of the post-intervention effect are broadly similar across the

two approaches, an important discrepancy emerges in the cumulative impact assessment. Specifically, the credible interval for the cumulative effect obtained with CausalImpact library does not include zero, suggesting a statistically significant intervention effect. In contrast, the corresponding credible interval derived from the Stan implementation does include zero, indicating greater posterior uncertainty and preventing a clear conclusion about the presence of a cumulative effect.

This difference likely reflects variations in prior specification, state component parameterization or posterior sampling behavior between the two implementations. The Stan model provides full control over hyperpriors and variance components, which may result in more conservative uncertainty quantification if weaker or more diffuse priors are used. Additionally, small differences in how the state-space components are initialized and constrained can propagate over time and affect cumulative uncertainty.

Overall, while both models suggest a similar direction of the intervention effect, the discrepancy in the cumulative credible intervals highlights the sensitivity of long-horizon impact estimates to modeling assumptions and prior choices.

4 Spatial Stan Model For Lombardy

After analyzing the intervention effect for the city of Milan, we extended the analysis to the entire Lombardy region in order to capture potential spatial heterogeneity that cannot be detected in a single-city framework. Focusing exclusively on Milan may overlook broader spatial dynamics in air pollution patterns, as neighboring areas can influence and be influenced by local environmental policies. Moving to a regional perspective, our objective was to model the spatial dependence structure across the monitoring stations and obtain a more comprehensive assessment of the impact of the intervention.

The dataset for the regional analysis was constructed following the same preprocessing steps adopted for the Milan model. Although Lombardy has 99 air quality monitoring stations in total, only 51 stations actively and continuously recorded data during the study period from the beginning of 2010 to the end of 2017. Therefore, our spatial analysis was based on these 51 stations, allowing for coherent temporal and spatial modeling without introducing additional missing-data complications.

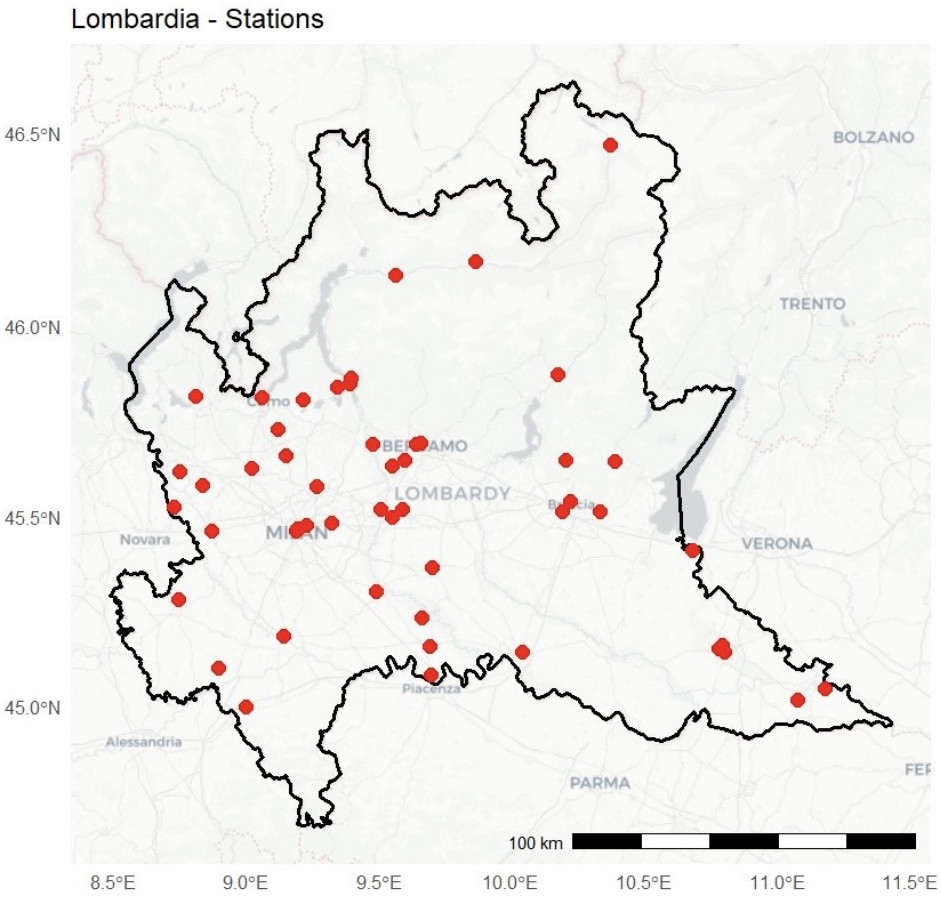

Figure 8: Map of the 51 ARPA stations in Lombardy that were active during our entire study period

4.1 Implementation

4.1.1 Initial Stan Model

We started our analysis with a multivariate spatio-temporal autoregressive regression model, designed to jointly capture temporal dependence, covariate effects, and spatial correlation across monitoring stations. Let $\mathbf{y}_t \in \mathbb{R}^M$ denote the vector of pollutant concentrations observed at time $t = 1, \ldots, 416$ across the $M = 51$ stations in Lombardy. Conditional on the previous observation $\mathbf{y}_{t-1}$, the regression coefficients, and the spatial random effects, the model assumes

$$\mathbf{y}_t | \alpha, \mathbf{y}_{t-1}, \boldsymbol{\beta}, \mathbf{w}, \Sigma \overset{\text{ind}}{\sim} \mathcal{N}_M\big(\alpha \mathbf{y}_{t-1} + \boldsymbol{\beta}\mathbf{X}_t + \mathbf{w}, \Sigma\big) \qquad t = 1, \ldots, 416$$

The term $\alpha \mathbf{y}_{t-1}$ introduces a first-order temporal autoregressive structure AR(1), with $\alpha \in (-1, 1)$. The matrix $\mathbf{X}_t$ contains the $K = 4$ covariates at time t (max and min temperature, sum of the weekly rain and max wind speed) and $\boldsymbol{\beta} \in \mathbb{R}^K$ represents their associated regression coefficients, capturing the effect of observed explanatory variables. The vector $\mathbf{w} \in \mathbb{R}^M$ models spatial random effects shared across time and accounts for residual spatial dependence not explained by the covariates or temporal dynamics.

The spatial effect is assumed to follow a multivariate normal distribution with exponential covariance matrix S_w:

$$\mathbf{w} \sim \mathcal{N}_M(\mathbf{0}, S_w), \qquad S_w(i, j) = \sigma_w^2 \exp\left(-\frac{\text{dist}(s_i, s_j)}{l}\right)$$

where s_i and s_j denote the spatial locations of stations i and j. This structure implies that correlation between stations decays exponentially with distance, with σ_w^2 controlling the marginal spatial variance and l governing the spatial range. l is fixed *a priori* and set equal to one third of the maximum inter-station distance. The variance parameter σ_w^2 is assigned an Inverse-Gamma$(2, 1)$ prior.

Then we set:

$$\boldsymbol{\beta} \sim \mathcal{N}_K(\mathbf{0}, I),$$

$$\alpha \sim \text{Uniform}(-1, 1)$$

$$\Sigma \sim \text{Inverse-Wishart}(M + 2, \Sigma_0),$$

where Σ_0 is equal to the empirical covariance matrix estimated from the data.

Overall, this hierarchical specification simultaneously models temporal persistence, covariate effects, spatial correlation through a structured Gaussian random field and cross-station residual dependence.

4.1.2 Changes to make the model computationally feasible

The initial stan model explained in the previous section is theoretically well-defined, but it was computationally infeasible in practice. The main difficulty came from presence of the Inverse-Wishart prior on the high-dimensional covariance matrix Σ. In particular, sampling from the Inverse-Wishart distribution becomes increasingly unstable and computationally demanding as the dimension M grows (we have $M = 51$), due to the strong coupling it induces among variance and correlation parameters and the poor geometry it generates for Hamiltonian Monte Carlo. This often leads to slow mixing, divergent transitions, and highly inefficient exploration of the posterior distribution.

Independent and identically distributed residuals. As a first simplification, we implemented a version of the model assuming independent and identically distributed residuals, i.e. $\Sigma = \sigma^2 I$. This modification dramatically reduced the computational burden, since only a single variance parameter needed to be estimated and no cross-station residual dependence was modeled. The model ran efficiently and converged without any issue. However, this assumption was overly restrictive, as it ignored contemporaneous correlation between nearby monitoring stations, therefore oversimplifying the spatial dependence structure and potentially underestimating uncertainty.

LKJ-distribution. To retain flexibility while improving computational stability, we replaced the Inverse-Wishart prior with a separation strategy based on an LKJ distribution for the correlation matrix. In particular, we decomposed Σ as

$$\Sigma = diag(\tau) \times \Omega \times diag(\tau),$$

where $diag(\tau)$ is a diagonal matrix of standard deviations and Ω is a correlation matrix. The standard deviations were assigned weakly informative priors, while the correlation matrix Ω was modeled using an LKJ(η) distribution [1]. The LKJ prior is defined directly on the space of valid correlation matrices and allows control over the strength of prior shrinkage toward the identity matrix: for $\eta = 1$ it is uniform over correlation matrices, while larger values of η increasingly concentrate prior mass around zero. This parameterization improves sampling efficiency by decoupling scale and correlation parameters and by inducing a more favorable posterior geometry for HMC.

Distance threshold. Finally, to reduce overparameterization, we imposed additional sparsity by constraining to zero the off-diagonal elements of Ω corresponding to pairs of stations separated by large distances. In practice, correlations were estimated only for geographically proximate stations, while distant stations were assumed conditionally independent at the residual level. The distance threshold was selected empirically: knowing that the maximum inter-station distance was 203 km, we initially set the threshold at 50 km and progressively increased it up to 100 km, at which point the model began to exhibit clear signs of computational deterioration, including much longer compilation times and a substantial reduction in the effective sample size (n_{eff}) of several parameters. The introduction of this distance threshold reduced the number of free parameters and enforced a spatially coherent dependence structure, leading to a model that was computationally feasible while still capturing the most relevant spatial interactions.

4.2 Posterior Analysis

We fitted the model only on the pre-intervation period, then we generated posterior predictive distributions for the counterfactual responses at each station during the post-intervention period. In particular, for each posterior draw of the parameters, we propagated the model forward recursively using the autoregressive structure and the estimated spatial effects, obtaining a full posterior distribution of the counterfactual PM10 concentrations.

Autoregressive component. We first analyzed the posterior distribution of the autoregressive parameter α. The posterior mass is concentrated away from zero and lies well within the stationarity region $(-1, 1)$ with 95% credible interval [0.42, 0.47], indicating strong temporal persistence in pollutant concentrations. This result confirms that past pollution levels are a key predictor of current values reflecting air quality dynamics, atmospheric accumulation and slow dispersion processes.

Regression coefficients. In contrast, the regression coefficients $\boldsymbol{\beta}$ associated with the observed covariates appear to have limited explanatory power. Their posterior distributions are generally centered close to zero, with credible intervals that include zero for most covariates. This suggests that, conditional on the autoregressive component and the spatial random effect, the contribution of the weather covariates is modest. This result is consistent with the analysis we performed before for the Milan station, where the only statistically significant regressor was the concentration of PM10 outside Area C, while the weather covariates were not significant.

Spatial random effects. Finally, the spatial random effects $\mathbf{w}$ reveal a clear geographical pattern (Figure 9). Posterior estimates indicate systematic differences between stations located in the northern part of the region and those in the central and southern areas. In particular, northern stations tend to exhibit lower spatial effect values compared to the rest of Lombardy. A plausible explanation lies in the distinct geographical and socio-economic characteristics of these areas: the northern part of the region is predominantly mountainous, which may facilitate pollutant dispersion and is generally characterized by lower industrial density and traffic intensity. In contrast, the central and southern areas largely coincide with the Pianura Padana, one of the most industrialized and densely populated areas in Italy, where atmospheric conditions and human activity contribute to higher baseline pollution levels.

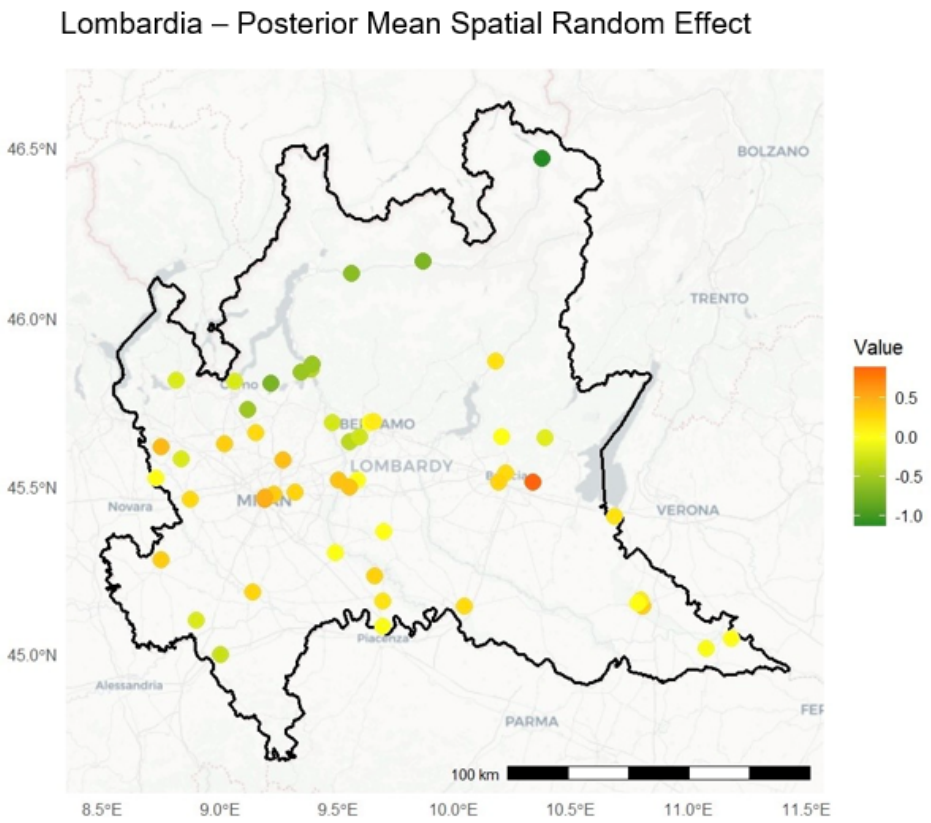

Figure 9: Map of Spatial random effects across stations

4.3 Cumulative Effect

To assess the spatial heterogeneity of the intervention, we computed the cumulative effect separately for each monitoring station. For every posterior draw, the cumulative effect at station i was calculated as

$$\text{CumEffect}_{i,T} = \sum_{t=t_0+1}^{T} \left(y_{i,t}^{\text{obs}} - y_{i,t}^{\text{cf}}\right), \qquad i = 1, \ldots, 51$$

where $t_0 = 106$ denotes the end of the pre-intervention period and $y_{i,t}^{\text{cf}}$ is the counterfactual prediction. This produces a full posterior distribution of the cumulative impact for each station, allowing both magnitude and uncertainty to vary spatially.

Figure 10 illustrates the posterior mean of the cumulative effect for each station over the post-intervention period. The plot highlights a clear spatial heterogeneity in the estimated intervention effect. In particular, the station located inside Area C has negative cumulative effect, indicating that observed pollution levels were, on average, lower than their counterfactual predictions. In contrast, the station located in Milan but outside Area C does not show the same pattern, consistently with the previous results from Causal Impact.

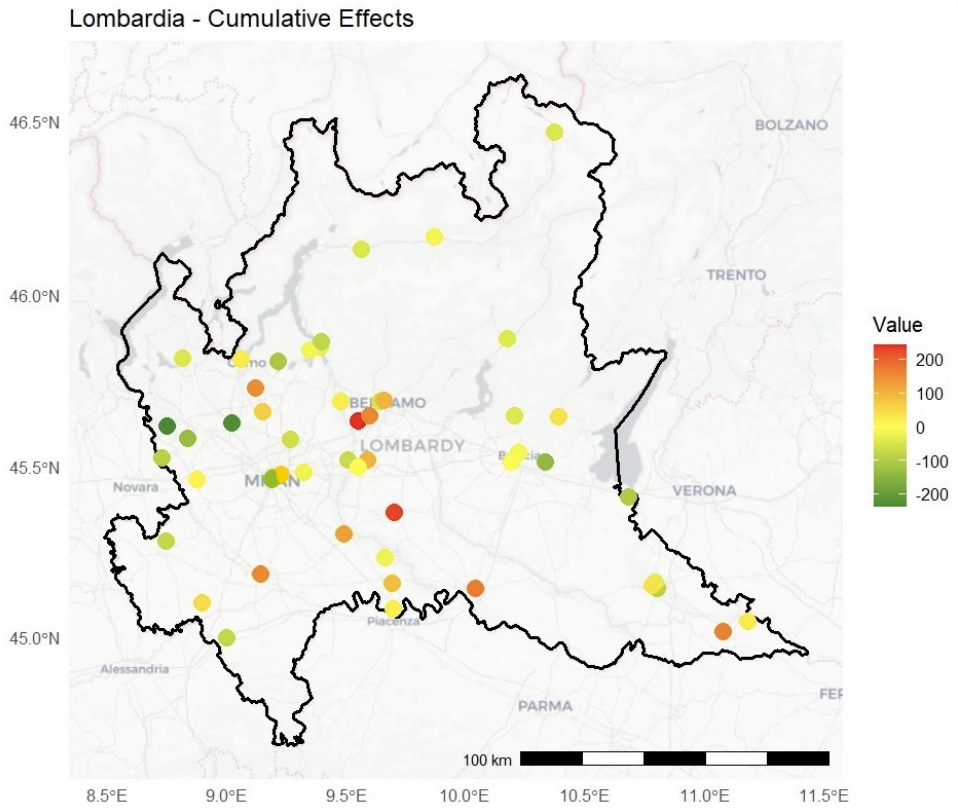

Figure 10: Map of cumulative sum of the effect across stations

Beyond Milan, several stations display negative cumulative effects even though they are not geographically close to Area C. This suggests that local dynamics unrelated to the policy, such as local environmental measures, traffic regulations or structural changes in emissions, may have contributed to reductions in those areas. The spatial dispersion of these negative effects indicates that the regional pollution dynamics are influenced by multiple factors and not only by a single centralized intervention.

At the same time, a number of stations, particularly those located in municipalities surrounding Milan, exhibit positive cumulative effects. One plausible interpretation is the presence of spatial spillover or displacement effects: the introduction of Area C may have reduced traffic and emissions within the restricted zone while partially redirecting traffic flows toward neighboring urban areas.

4.4 Posterior probability of an effect

In addition to analyzing the magnitude of the cumulative effects, we computed the posterior probability of an intervention effect for each station. This choice was motivated by the desire to recall and mirror one of the key summary measures provided by the `CausalImpact` framework, namely the posterior probability that the intervention had a non-zero effect.

For each station, the posterior probability of an effect was calculated as the proportion of posterior draws in which the cumulative effect had a consistent sign. More precisely,

letting $\{\text{CumEffect}_i^{(s)}\}_{s=1}^{S}$ denote the posterior draws of the cumulative effect for station i, we computed

$$p_i = \max\left(\frac{1}{S}\sum_{s=1}^{S}\mathbb{I}\left(\text{CumEffect}_i^{(s)} > 0\right),\ \frac{1}{S}\sum_{s=1}^{S}\mathbb{I}\left(\text{CumEffect}_i^{(s)} < 0\right)\right),$$

This quantity represents the posterior probability that the cumulative effect is either strictly positive or strictly negative. Following the rule used by `CausalImpact`, we considered the evidence for an intervention effect to be strong when this probability is above 95%.

Figure 11 displays the resulting percentages for all stations, distinguishing those above and below the 95% threshold. This visualization provides an immediate assessment of where the model assigns strong posterior support to a systematic deviation from the counterfactual trajectory, and where the evidence remains inconclusive.

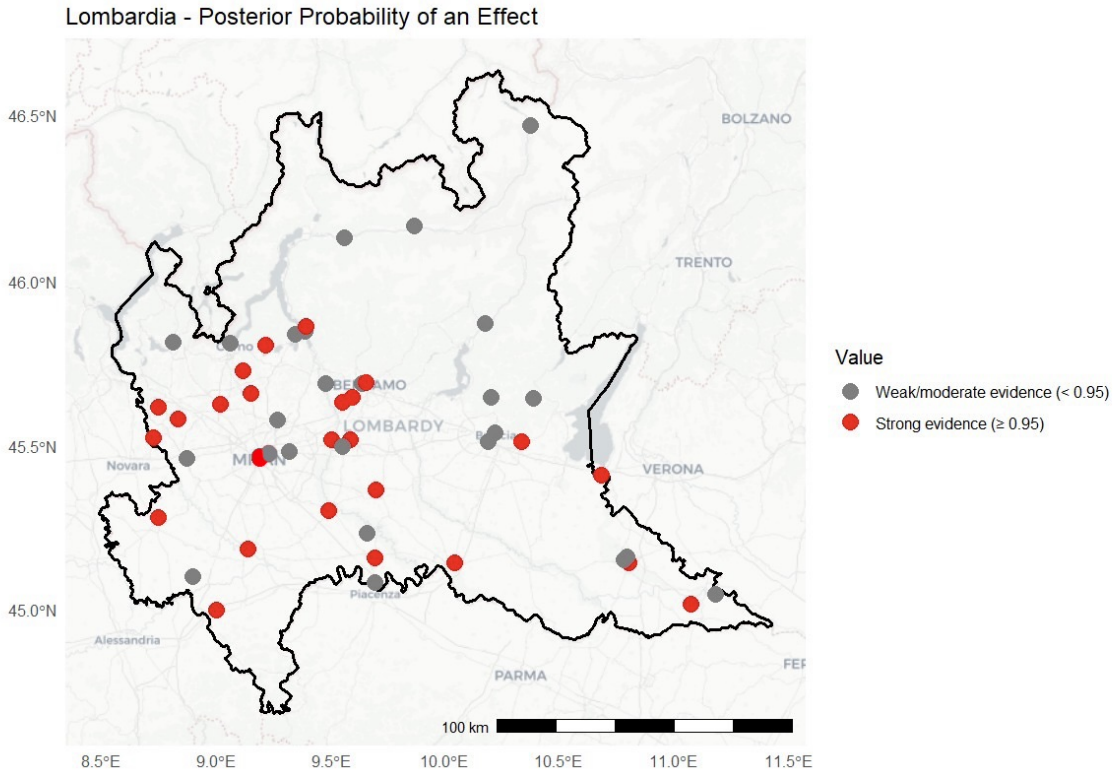

Figure 11: Map of Posterior probability of an effect across stations

The spatial distribution of strong evidence closely aligns with the patterns observed in the cumulative mean effects: the intervention appears to have had a localized impact within Area C, while regional pollution dynamics display substantial spatial heterogeneity that cannot be attributed solely to this policy.

5 Conclusions

Our analysis combined a city-level causal inference approach with a regional spatio-temporal model to evaluate the impact of the introduction of Area C on air pollution levels. The Milan-only analysis, implemented both through the `CausalImpact` package and a custom Stan model replicating its structure, provided initial evidence of a localized intervention effect. While the two implementations produced broadly consistent point estimates, differences in uncertainty quantification highlighted the sensitivity of cumulative conclusions to prior specification and modeling choices.

Extending the analysis to the entire Lombardy region allowed us to account explicitly for spatial dependence and heterogeneity across monitoring stations. The hierarchical spatio-temporal model captured strong temporal persistence, limited additional explanatory power from observed weather covariates and relevant spatial structure. This broader perspective revealed that pollution dynamics are shaped not only by the intervention but also by persistent territorial characteristics and regional interactions.

The station-specific cumulative effects showed that both negative and positive values were observed across the region, suggesting that additional local factors influenced air quality during the post-intervention period. The posterior probability analysis reinforced these results.

Overall, the results suggest that Area C had a measurable and geographically concentrated impact on pollution levels within the restricted zone in Milan. However, the regional analysis indicates that air quality dynamics are driven by a complex combination of policy interventions, spatial dependence and local structural conditions. This highlights the importance of adopting a spatially explicit modeling framework when evaluating urban environmental policies, as city-level analysis alone may not fully capture regional heterogeneity.

References

[1] Stan User's Guide. Multivariate priors for hierarchical models. https://mc-stan.org/docs/stan-users-guide/regression.html#multivariate-hierarchical-priors.section.

[2] Jim Koehler Nicolas Remy Kay H. Brodersen, Fabian Galluser and Steven L. Scott. Inferring causal impact using bayesian structural time-series models. *The Annals of Applied Statistics*, 9(1):247–274, 2015.

[3] Open-Meteo. Historical weather api. https://open-meteo.com/en/docs/historical-weather-api?start_date=2020-01-18&hourly=&daily=temperature_2m_max,temperature_2m_min,rain_sum,wind_speed_10m_max.

[4] Regione Lombardia. Dati sensori aria 2010-2017. https://www.dati.lombardia.it/Ambiente/Dati-sensori-aria-2010-2017/nr8w-tj77/about_data.

[5] Regione Lombardia. Stazioni qualità dell'aria. https://www.dati.lombardia.it/Ambiente/Stazioni-qualit-dell-aria/ib47-atvt/about_data.

GitHub Repository: https://github.com/marymazza/BayesianStatisticsProject